The vnd/NK-2 Homeodomain: Thermodynamics of Reversible Unfolding and DNA Binding for Wild-Type and with Residue Replacements H52R and H52R/T56W in Helix III

Martin Gonzalez,[‡] Solly Weiler,[§,||] James A. Ferretti,[§] and Ann Ginsburg*[,‡]

Section of Protein Chemistry, Laboratory of Biochemistry, and Laboratory of Biophysical Chemistry, National Heart, Lung and Blood Institute, National Institutes of Health, Bethesda, Maryland 20892

Received September 22, 2000; Revised Manuscript Received January 17, 2001

ABSTRACT: The conformational stabilities of the vnd (ventral nervous system defective)/NK-2 homeodomain [HD(wt); residues 1−80 that encompass the 60-residue homeodomain] and those harboring mutations in helix III of the DNA recognition site [HD(H52R) and HD(H52R/T56W)] have been investigated by differential scanning calorimetry (DSC) and ellipticity changes at 222 nm. Thermal unfolding reactions at pH 7.4 are reversible and repeatable in the presence of 50−500 mM NaCl with $\Delta C_p = 0.52 \pm 0.04$ kcal K^{-1} mol^{-1}. A substantial stabilization of HD(wt) is produced by 50 mM phosphate or by the addition of 100−500 mM NaCl to 50 mM Hepes, pH 7.4, buffer (from $T_m = 35.5$ °C to T_m 43−51 °C; $\Delta H_{vH} \cong 47 \pm 5$ kcal mol^{-1}). The order of stability is HD(H52R/T56W) > HD(H52R) > HD(wt), irrespective of the anions present. Progress curves for ellipticity changes at 222 nm as a function of increasing temperature are fitted well by a two-state unfolding model, and the cooperativity of secondary structure changes is greater for mutant homeodomains than for HD(wt) and also is increased by adding 100 mM NaCl to Hepes buffer. A 33% quench of the intrinsic tryptophanyl residue fluorescence of HD(wt) by phosphate binding ($K_D' = 2.6 \pm 0.3$ mM phosphate) is reversed ~60% by DNA binding. Thermodynamic parameters for vnd/NK-2 homeodomain proteins binding sequence-specific 18 bp DNA have been determined by isothermal titration calorimetry (10−30 °C). Values of ΔC_p are +0.25, −0.17, and -0.10 ± 0.04 kcal K^{-1} mol^{-1} for HD(wt), HD(H52R), and HD(H52R/T56W) binding duplex DNA, respectively. Interactions of homeodomains with DNA are enthalpically controlled at 298 K and pH 7.4 with corresponding ΔH values of -6.6 ± 0.5, -10.8 ± 0.1, and -9.0 ± 0.6 kcal mol^{-1} and $\Delta G'$ values of -11.0 ± 0.1, -11.0 ± 0.1, and -11.3 ± 0.3 kcal mol^{-1} with a binding stoichiometry of 1.0 ± 0.1. Thermodynamic parameters for DNA binding are not predicted from homeodomain structural changes that occur upon complexing to DNA and must reflect also solvent and possibly DNA rearrangements.

The homeodomain is the highly conserved DNA-binding domain of a class of proteins that function as transcriptional regulators, specifying positional and temporal information in the commitment of embryonic cells to specific developmental pathways. An early step in the cascade of events associated with development is the sequence-specific binding of the transcriptional regulator, i.e., the homeodomain-containing protein, to a specific sequence or a specific set of sequences of DNA (*1*−*3*). Various genetic diseases and developmental abnormalities have been mapped to base changes in a homeobox, the gene that encodes the homeodomain protein (*4*−*7*). Such mutations often alter structural stability, DNA recognition specificity, or binding affinity of the homeodomain for DNA (*8*−*10*).

The homeodomain studied here is encoded by the *vnd* (ventral nervous system defective)/NK-2 gene of *Drosophila melanogaster* (*11*−*13*) and is the parent member of the vnd/NK-2[1] class of homeodomains first described by Kim and Nirenberg (*11*). The availability of the NMR solution structures of the free and DNA-bound forms of the vnd/NK-2 homeodomain determined by Tsao et al. (*14*, *15*) and Gruschus et al. (*16*) permits identification of those amino acid residues that interact with DNA. Moreover, the effects of amino acid replacements in the vnd/NK-2 homeodomain have been studied and give valuable information on both the stability and changes in the affinity for sequence-specific 18 bp DNA based on electrophoretic mobility shift assays (*8*). To complement structural studies, the conformational

* To whom correspondence should be addressed at NHLBI/NIH, Building 3, Room 208, Bethesda, MD 20892-0342. E-mail: aog@cu.nih.gov. Fax: 301-496-0599. Tel: 301-496-1278.

[‡] Section of Protein Chemistry, Laboratory of Biochemistry.

[§] Laboratory of Biophysical Chemistry.

[||] Present address: Howard Hughes Medical Institute, Dana-Farber Cancer Institute, 1 Jimmy Fund Way, SM 758, Boston, MA 01772.

[1] Abbreviations: vnd/NK-2, ventral nervous system defective/NK-2 homeodomain protein; HD(wt), wild-type vnd/NK-2 homeodomain; HD(H52R), vnd/NK-2 homeodomain in which His52 has been replaced by Arg; HD(H52R/T56W), vnd/NK-2 homeodomain in which both His52 and Thr56 have been replaced by Arg and Trp, respectively; Hepes, *N*-(2-hydroxyethyl)piperazine-*N*′-2-ethansulfonic acid; DSC, differential scanning calorimetry; CD, far-UV circular dichroism in molar ellipticity units; ITC, isothermal titration calorimetry; ΔH_{cal}, calorimetric enthalpy; T_m, midpoint transition temperature for the unfolding/refolding process; ΔC_p, heat capacity change; ΔH_{vH}, van't Hoff enthalpy for two-state, reversible protein unfolding; NATA, *N*-acetyltryptophanamide.

10.1021/bi0022341 CCC: $20.00
Published on Web 03/28/2001

stabilities of the wild-type homeodomain [HD(wt)] and those with one and two amino acid residue replacements in the DNA binding region of the NK-2 homeodomain [HD(H52R) and HD(H52R/T56W)] have been studied here by differential scanning calorimetry and far-UV circular dichroism as a function of buffer/salt composition. Tertiary structural changes have been monitored by second derivative UV absorbance and fluorescence measurements. Isothermal titration calorimetry has been used to determine apparent association constants and enthalpic changes upon vnd/NK-2 homeodomains forming 1:1 complexes with sequence-specific 18 or 28 bp DNA under different ionic conditions at pH 7.4.

MATERIALS AND METHODS

Chemicals. Hepes (Sigma), salts, and other reagents were of analytical grade. All aqueous solutions were prepared with distilled water that was deionized and filtered through a Millipore MilliQ-UV-Plus reagent-grade system. This water also was used for rinsing glassware and for cleaning calorimeter cells.

DNA. Single-strand 18 base DNA, 5′-TGTGT**CAAGTG**-GCTGTAG-3′, and its complementary, 5′-CTACAGCCACT-TGACACA-3′, and single-strand 28 base DNA, 5′-GGC-CGTGTGT**CAAGTG**GCTGTAGGCGCG-3′, and the complementary, 5′-CGCGCCTACAGCCACTTGACACACG-GCC-3′, containing the vnd/NK-2 target site (5′-**CAAGTG**-3′) as part of the core, were synthesized and purified by Midland Certified Reagent Co. (Midland, TX). The purity of the strands was checked by mass spectroscopy. The corresponding duplex (18 or 28 bp) DNA oligomers were prepared by mixing equal molar amounts of the appropriate single strands from stock solutions of ∼24 mg/mL in water and annealing by heating for 4 min at 95 °C and slowly cooling to 4 °C. Annealing was checked by agarose gel electrophoresis, and proton NMR was used to check the core structures. DNA stock solutions in water (∼3 mM) were stored at −20 °C. Concentrations of dialyzed, diluted duplex DNA for ITC experiments were determined by absorbances at 260 nm (ϵ = 193 000 and 289 000 M^{-1} cm^{-1} for 18 and 28 bp DNA with corresponding M_r of 11 000 and 17 180, respectively).

Protein Expression and Purification. Each 80 amino acid residue protein that contains the vnd/NK-2 homeodomain HD(wt), HD(H52R), or HD(H52R/T56W) was cloned in the expression vector pET15b and overexpressed in *Escherichia coli* growing in a LB−ampicillin−chloramphenicol medium after inducing expression with isopropyl β-D-thiogalactoside (*17*) as described by Weiler et al. (*8*). Cells were harvested and resuspended in buffer A containing 5 mM imidazole, 500 mM NaCl, and 20 mM Tris-HCl (pH 7.9). Purification steps were as described by Xiang et al. (*9*). Purified proteins were dialyzed against water, lyophilized, and stored at −20 °C. Proteins were homogeneous by SDS gel electrophoresis and mass spectroscopy, which also yielded molecular weights for HD(wt), HD(H52R), and ^{15}N-labeled HD(H52R/T56W) of 9693.7 ± 0.7, 9713.0 ± 1.1, and 9936.0 ± 1.4, respectively. Molecular weights calculated from the amino acid sequences (*11*) were 9694, 9713, and 9927 for HD-(wt), HD(H52R), and ^{15}N-labeled HD(H52R/T56W), respectively. Corresponding molar extinction coefficients were calculated from 5550∑Trp +1340∑Tyr + 150∑Cys (*18*). Calculated values of ϵ (specific absorbance) at 280 nm were 10 910 M^{-1} cm^{-1} (1.13 cm^2/mg), 10 910 M^{-1} cm^{-1}(1.12 cm^2/mg), and 16 460 $M^{-1}cm^{-1}$ (1.66 cm^2/mg) for HD(wt), HD-(H52R), and HD(H52R/T56W), respectively, and these values were used for calculating protein concentrations from absorbance measurements at 280 nm.

Differential Scanning Calorimetry. DSC measurements utilized the VP-DSC of Plotnikov et al. (*19*) from MicroCal, Inc., Northampton, MA. Instrument calibrations were performed as previously described (*20*). The VP-DSC was run without feedback and with a 30 min preequilibration time (usually at 15 °C) before the first scan; for experiments in which two or more consecutive scans were set up, the interval between scans was extended to ∼2 h. Before DSC runs, protein samples were thoroughly dialyzed in the appropriate buffers, and the instrument baseline was determined by scanning the dialysate buffer in both the sample and reference cells of the VP-DSC instrument at the scan rate to be used for the protein. Buffer and protein solutions were thoroughly degassed prior to loading into the cells. DSC data obtained for the protein in the sample cell vs dialysate in the reference cell were corrected for the instrument baseline, normalized for a scan rate of 60 °C/h, and moles of protein in the sample cell (0.5114 mL). DSC profiles were analyzed with either the calorimetry software from ORIGIN-MicroCal, Inc., or the EXAM program of Kirchhoff (*21*), which yielded areas of endotherms after pre- and posttransition baselines were subtracted (ΔH_{cal}) and calculated van't Hoff enthalpies (ΔH_{vH}). Protein concentrations were 30−50 μM for DSC measurements, although 20 or 90 μM homeodomain was used in some experiments. Enthalpy values are expressed in kilocalories per mole, where 1.000 cal = 4.184 J.

Circular Dichroism. Circular dichroism measurements were made using a Jasco-710 spectropolarimeter with an attached Neslab RT-110 circulating bath and controlled by the computer software. Buffer contributions to protein CD spectra (in the same cell) were determined both before and after protein spectra and were subtracted from the protein CD spectra. Changes in the ellipticity [θ] of the protein at 222 nm, as a function of temperature, were performed with protein concentrations of ∼0.4 mg/mL in a jacketed, cylindrical cell having 0.05 cm path length. The experimental results are expressed as mean residue molar ellipticity units (deg cm^2 $dmol^{-1}$), using mean residue molecular weights of 119.68 for HD(wt), 119.91 for HD(H52R), and 122.55 for the ^{15}N-labeled HD(H52R/T56W). Thermal unfolding experiments were performed at a scan rate of 60 °C/h from 10 to 80 °C; a second cycle of heating was made 2 h after the sample was rapidly cooled to 10 °C. CD data were analyzed by fitting to a two-state model of unfolding using the EXAM program (*21*). Equilibrium CD measurements were performed by waiting for the protein in the cell to reach a time-independent ellipticity value (∼15 min) after temperature increases in 5 °C increments.

Isothermal Titration Calorimetry. The VP-ITC microcalorimeter (MicroCal, Inc., Northampton, MA) was used as recommended by the manufacturer. Running temperatures were 10 to 35 °C. In typical experiments, 15−18 consecutive injections of 5 μL aliquots of 35−65 μM protein solutions were injected from the syringe into the reaction cell (1.4061 mL) containing 0.9−1.6 μM sequence-specific 18 or 28 bp duplex DNA. The duration of each injection was according

to the volume added (2 s/μL of injectant), and injections were made at intervals of 5 or 7 min. The DNA solution was maintained at a constant stirring speed of 300 rpm in order to ensure proper mixing after each protein injection. A first injection of <10% of later injection volumes was made for each titration in order to avoid artifacts arising from a bubble and/or diffusion from the syringe tip during temperature equilibration (*22*). Dilution heats of protein into DNA solutions (which agreed with those obtained by injections of proteins into the same volume of buffer) were subtracted from measured heats of binding. Both the protein and DNA solutions were dialyzed in separate Slide-A-Lyzer Cassettes (1000 MW cutoff, Pierce) against the same buffer prior to ITC experiments to ensure chemical equilibration. Some instability of dilute, dialyzed DNA solutions stored at 4 °C between ITC experiments was apparent, which introduced an error into calculations of the stoichiometry of protein−DNA complex formation ($n = 1.0 \pm 0.1$). The binding enthalpy was calculated from the average of the measured heats for the first 2−9 injections in each experiment when duplex DNA was in molar excess of the homeodomain. ITC titration data were analyzed with the Origin program provided by Micro-Cal, Inc.

Second Derivative UV Spectral Measurements. Second derivative UV spectral measurements as a function of temperature were performed using a diode array Hewlett-Packard 8453 spectrophotometer with a peltier temperature control device (*23*, *24*). Each second derivative spectrum was an average of 10 spectra and was obtained by heating the sample (~0.2 mg/mL) in a microcell (100 μL volume, 1 cm path length). Spectra were taken between 275 and 300 nm, every 5 deg from 20 to 75 °C, after equilibration at each temperature for 10 min.

Fluorescence Spectroscopy. Fluorescence measurements were performed in a SLM Aminco-Bowman Series 2 spectrofluorometer attached with a programmable water-circulating bath, Neslab RT-111. Measurements were taken using polarizers positioned at 54.7° in the emission light beam and 0° for the excitation. Excitation was at 295 nm, with 4 nm slits for both excitation and emission. Water-jacketed cuvettes (1 mL, 1 cm path length) were connected to the circulating bath. The temperature inside the sample cuvette was monitored with a microthermocouple (Omega Inc., Stamford, CT) inserted into a cell (containing water) in tandem with the sample cuvette. Titrations of HD(wt) (18 μM concentration in water or 50 mM Hepes ± NaCl, pH 7.4, buffer at 20 °C) with sodium phosphate were performed by addition of small aliquots from a 1 M sodium phosphate solution stock, pH 7.4. For the titration of HD(wt) with sodium phosphate followed by the addition of an equimolar amount of 28 bp DNA (1.64 mM stock solution), corrections for the buffer baseline, dilution, and inner filter effect were made (*25*). Procedures and assumptions in the data treatment for the calculation of an apparent K_D' for sodium phosphate are described in Ginsburg et al. (*26*).

RESULTS

Thermal Unfolding Studies. The conformational stabilities of the wild-type protein, HD(wt), as well as HD(H52R) and HD(H52R/T56W) of the vnd/NK-2 homeodomain have been investigated by far-UV circular dichroism and differential scanning calorimetry.

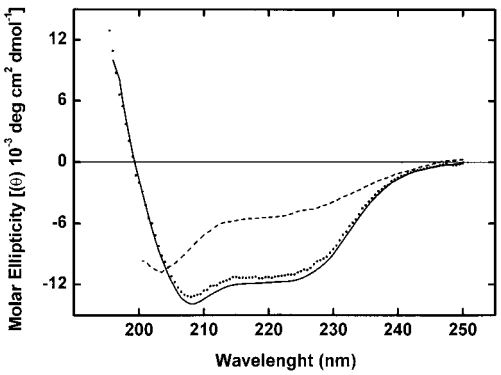

FIGURE 1: Far-UV circular dichroism spectra for the HD(H52R) protein in 50 mM sodium phosphate/100 mM NaCl, pH 7.4, buffer. CD spectra of the protein (0.37 mg/mL) at 10 °C (solid line), at 80 °C after heating from 10 at 60 °C/h (dashed line), and after rapid cooling of the sample from 80 °C and equilibrating for 2 h at 10 °C (dotted line).

Far-UV circular dichroism spectra are shown for the HD(H52R) protein in 50 mM sodium phosphate/100 mM NaCl, pH 7.4, at 10 °C before heating (solid line in Figure 1), at 80 °C (dashed line), and after cooling to 10 °C for 2 h (dotted line). A second heating from 10 to 80 °C followed by cooling gave the same spectra as obtained for the first cycle (data not shown). Thus, the secondary structure of the HD(H52R) protein is disrupted by heating, and the folded form is regained upon cooling. The same far-UV CD spectra and reversibility are obtained with HD(wt) and HD(H52R/T56W). The far-UV CD spectrum for the folded form of the vnd/NK-2 homeodomain in sodium phosphate buffer is similar to that reported by Damante et al. (*27*) for the TTF-1 homeodomain, which also has the helix−turn−helix DNA binding motif.

Progress curves for ellipticity changes at 222 nm as a function of increasing temperature are shown in Figure 2 (panels A, B, and C) for HD(wt) in 50 mM Hepes, pH 7.4, buffer containing 0, 100 mM, and 500 mM NaCl, respectively. In the absence of NaCl, hysteresis during refolding of HD(wt) occurs. The presence of NaCl apparently is necessary for correct refolding (within 2 h at 10 °C) after heating to 80 °C (compare panels B and C with panel A in Figure 2). During refolding in the presence of NaCl after rapid cooling from high temperatures, a return to the initial ellipticity values at 10 °C has been observed to take as long as 1.5 h when the CD signal was monitored as a function of time. However, equilibrium CD measurements (during which the CD signal is monitored at 5 °C increments of increasing temperatures until time-independent changes are complete: 12−15 min) for HD(wt) under the conditions of Figure 2B give essentially the same results as obtained at a heating rate of 60 °C/h (data not shown). Thus, an equilibrium between folded and unfolded states of the protein occurs from 20 to 80 °C when scanned at a rate of 60 °C/h when 100 mM NaCl is present. CD data for the first and second cycles of heating are fitted well to a two-state unfolding model (Figure 2, overlaid solid curves). Parameters of these fits as well as those obtained by fitting progress curves of CD changes at 222 nm as a function of increasing temperature for HD(wt) and both HD(H52R) and HD(H52R/T56W) proteins under various ionic conditions are given in Table 1. Values of T_m from DSC and ellipticity changes at 222 nm at a scan rate of 60 °C/h agree.

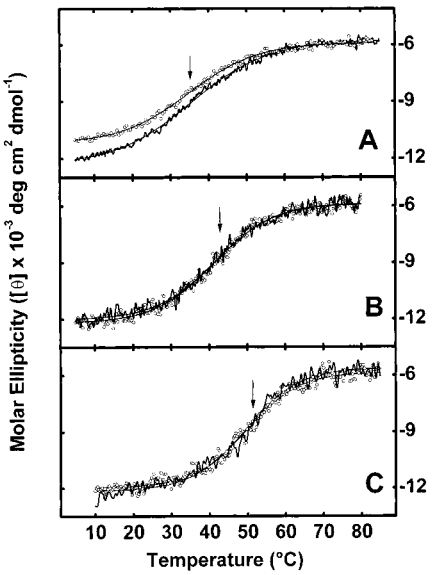

FIGURE 2: Progress curves for ellipticity changes at 222 nm as functions of increasing temperature for 0.42 mg/mL HD(wt) in 50 mM Hepes, pH 7.4, buffer in the absence of NaCl (A) and the presence of 100 mM NaCl (B) and 500 mM NaCl (C). In each panel (A, B, or C), CD values are connected by a heavy solid line for the first heating cycle whereas open circles correspond to a second heating cycle; thin solid curves show superimposed fits of CD data to a two-state unfolding model. The arrows indicate the midpoint denaturation temperatures (see Table 1).

The HD(H52R) and HD(H52R/T56W) proteins have an ion pair interaction between Glu17 and Arg52 that is not present in the wild-type vnd/NK-2 homeodomain (*8*). This additional salt bridge apparently stabilizes these proteins as shown by transition temperatures being higher than T_m values of HD(wt) under the same buffer conditions (Table 1).

DSC experiments have been performed with HD(wt), HD(H52R), and HD(H52R/T56W). To investigate the effect of buffer salts on homeodomain stability, proteins have been heated in either 50 mM Hepes/NaOH or 50 mM sodium phosphate buffer at pH 7.4 containing various concentrations of NaCl. Reiterative DSC heating cycles (following rapid cooling and equilibration at 15 °C for 2 h) show no significant change in areas or shapes of endotherms. This is illustrated in Figure 3A, which shows raw data from three consecutive DSC scans of the HD(H52R) protein in 50 mM sodium phosphate/50 mM NaCl, pH 7.4, buffer and the reproducibility of the endotherm in the three cycles of heating. The absence of shifts in the posttransitional baselines indicates that aggregation or self-association does not occur. Moreover, the denaturation temperature is scan rate (30−60 °C/h) and concentration (~0.2−0.9 mg/mL) independent. Reversibility also has been tested by stopping DSC scans at <50% completion of endotherms followed by scanning the full temperature range which gives superimposed DSC profiles (*28*, *29*).

Figure 3B shows the first DSC scan for HD(H52R) after normalization for scan rate and protein concentration and a sigmoidal baseline connecting pre- and posttransitional baselines for nonzero ΔC_p. The data have been fitted both to a two-state model (dotted line in Figure 3B) or to a nonideal (non-two-state model; dashed line) with $\Delta C_p = 0.4 \pm 0.1$ kcal K^{-1} mol^{-1}, $\Delta H_{cal} = 34$ kcal mol^{-1}, $\Delta H_{vH} = 48$ kcal mol^{-1}, and $T_m = 55.5$ °C. The observed endotherms

Table 1: Thermodynamic Data from DSC and CD Experiments at pH 7.4[a]

protein	buffer salts[b]	method	T_m (°C)	ΔH_{cal} (kcal mol^{-1})	ΔH_{vH} (kcal mol^{-1})	CR[c]
HD(wt), ~50 μM	A + 0 mM NaCl	DSC	48.1	18	43	0.42
		CD	47.9		26	
	A + 200 mM NaCl	DSC	49.8	28	44	0.64
		CD	50.2		33	
	B + 0 mM NaCl	DSC[d]	35.5	11	43	0.27
		CD	35.8		19	
	B + 100 mM NaCl	DSC[d]	43.0	20	47	0.42
		CD	43.0		34	
		CD[e]	43.0		25	
	B + 500 mM NaCl	DSC[d]	51.2	34	50	0.68
		CD	52.0		42	
HD(H52R), ~40 μM	A + 0 mM NaCl	DSC	55.8	21	52	0.42
		CD	56.3		42	
	A + 50 mM NaCl	DSC	55.5	34	48	0.71
		CD	55.7		38	
	A + 100 mM NaCl	DSC	56.1	35	48	0.73
		CD	55.8		47	
	B + 0 mM NaCl	DSC	42.2	21	40	0.53
		CD	41.6		34	
	B + 100 mM NaCl	CD	51.2		46	
	B + 100 mM KCl	DSC	50.4	36	48	0.75
		CD	50.3		45	
HD(H52R/T56W), ~30 μM	A + 0 mM NaCl	DSC	58.0	30	54	0.55
		CD	55.5		44	
	B + 0 mM NaCl	DSC	44.5	27	44	0.61
		CD	42.1		32	
	B + 100 mM NaCl	DSC	57.6	44	55	0.80
		CD	55.2		54	

[a] Standard errors are $T_m \pm 0.2$ °C and $\Delta H \pm 8\%$. DSC data have been fitted to a non-two-state model, whereas CD data have been fitted to an ideal two-state unfolding model (see text). [b] Buffers, pH 7.4 (at ~25 °C), are as follows: A, 50 mM sodium phosphate; B, 50 mM Hepes, in the absence and presence of the indicated neutral salt concentrations. [c] CR is the cooperative ratio, $\Delta H_{cal}/\Delta H_{vH}$. [d] This DSC data set gives a value for $\Delta C_p = 0.52 \pm 0.04$ kcal K^{-1} mol^{-1} (Figure 4). [e] From equilibrium CD measurements.

for NK-2 homeodomain proteins HD(wt), HD(H52R), and HD(H52R/T56W) occur over a more narrow temperature range than predicted for two-state unfolding, which indicates that either intermolecular cooperativity (in the absence of irreversible self-association) or some unusual intramolecular process occurs during the thermal unfolding process (i.e., $\Delta H_{cal}/\Delta H_{vH}$ ratio ≤ 1.0; see below).

A better estimate of the ΔC_p value has been obtained with HD(wt) and increasing concentrations of NaCl, which markedly stabilize the protein in 50 mM Hepes/NaOH buffer at pH 7.4. The T_m value is increased from 35.5 °C to 43.0 and 51.2 °C in the presence of 100 and 500 mM NaCl, respectively, as shown by maxima in DSC endotherms (Figure 4). A plot of T_m values vs the calculated values of ΔH_{vH} from A, B, and C in Figure 4 (inset) gives a straight line with a slope (ΔC_p) equal to 0.52 ± 0.04 kcal K^{-1} mol^{-1}. This ΔC_p value agrees with that estimated for HD(H52R) from DSC (Figure 3B) and also indicates that ΔC_p is not affected by the presence of NaCl.

Values of ΔH_{vH} from DSC profiles are based on the ratio of the maximum peak height to the area of the transition curve over the sigmoidal baseline (*20*, *30*), and the average of these values is 47 ± 5 kcal mol^{-1} for the three homeodomain proteins in different buffers (Table 1). In contrast, fits of CD data to a two-state model of unfolding show that the cooperativity of unfolding secondary structures

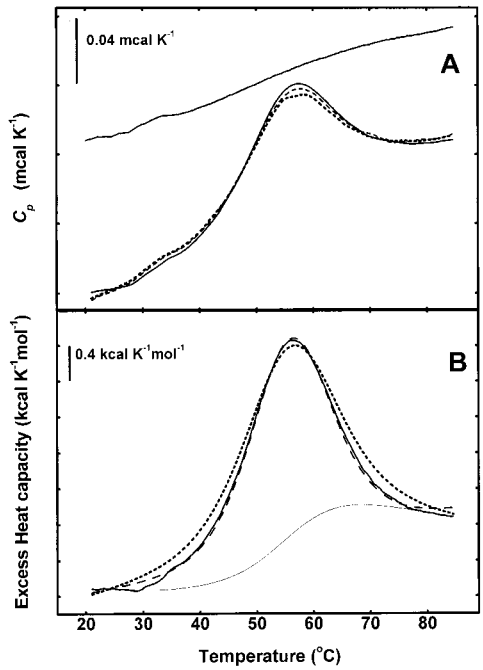

FIGURE 3: Differential scanning calorimetry. Panel A: DSC data for three consecutive scans of the HD(H52R) protein (0.54 mg/mL) in 50 mM sodium phosphate/50 mM NaCl, pH 7.4, buffer at a scan rate of 60 °C/h. The sample was cooled for 2 h at 15 °C between scans; first scan (solid curve), second scan (dashed curve), and third scan (dotted curve). The instrument baseline (buffer vs buffer) is shown by the top sloping line. Panel B: First scan (solid line) from panel A after subtracting the instrument baseline and normalizing for scan rate and protein concentration. A progress baseline has been fitted to the DSC profile and is shown connecting pre- and posttransitional baselines, which illustrates that $C_p > 0$. The DSC data are fitted better to a non-two-state model with $\Delta C_p = 0.4$ kcal K^{-1} mol^{-1} (dashed curve) than to an ideal two-state model (dotted curve) with the same ΔC_p value; see Table 1 for DSC parameters.

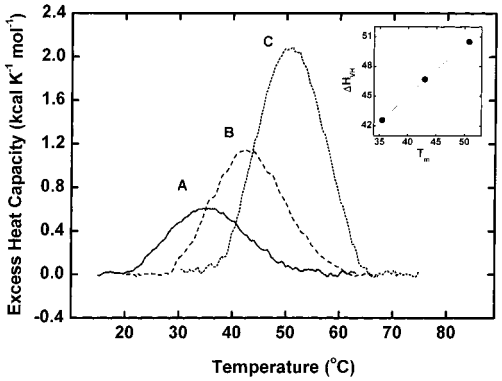

FIGURE 4: Stabilization of HD(wt) by increasing NaCl concentrations. DSC profiles of 0.39 mg/mL HD(wt) in 50 mM Hepes (pH 7.4) with 0 NaCl (A), 100 mM NaCl (B), and 500 mM NaCl (C) after subtraction of the instrument and progress baselines (see Figure 1). Inset: Plot of calculated ΔH_{vH} vs T_m values with a slope of 0.52 ± 0.04 kcal K^{-1} mol^{-1} for ΔC_p; see Table 1.

is in the order HD(wt) < HD(H52R) < HD(H52R/T56W), as reflected by corresponding ΔH_{vH} values in Table 1. In addition, the CD data of Table 1 indicate that the cooperativity of unfolding secondary structures in the wild-type and mutant vnd/NK-2 homeodomains is increased in each case by 100 mM NaCl in Hepes buffer or 50 mM sodium phosphate. The trend of ΔH_{cal} values from DSC under the different ionic conditions is similar to ΔH values obtained from CD although the magnitude of ΔH_{cal} values are lower.

The most striking feature of the data presented in Table 1 is the substantial stabilization of the wild-type NK-2 homeodomain and both HD(H52R) and HD(H52R/T56W) proteins by phosphate (12−14 °C). The presence of 100−500 mM NaCl in Hepes, pH 7.4, buffers also stabilizes the homeodomain proteins, whereas the addition of NaCl to phosphate, pH 7.4, buffer has little additional stabilizing effect. The substitution of KCl for NaCl has been found to severely impair the ability of the wild-type and both HD(H52R) and HD(H52R/T56W) proteins to refold, although almost the same thermodynamic parameters are observed for the first heating in the presence of KCl as with NaCl. Possibly, K^+ exerts a steric hindrance and/or unfavorable change in solvation water during refolding or Na^+ promotes correct refolding of the vnd/NK-2 homeodomain protein by specific binding.

Tertiary Structural Properties and Stability. Tryptophan residue 48 is conserved within the "DNA recognition helix" of all classical homeodomains. Trp48 in helix III has its indole ring extended toward helix I and perpendicular to the helix I axis (see Figure 8 below). Maxima in the intrinsic Trp fluorescence emission (with excitation at 295 nm) for HD(wt) or HD(H52R) in the presence of Hepes, phosphate, or DNA occur at 343 nm. A titration of HD(wt) in Hepes buffer, pH 7.4 at 20 °C, with sodium phosphate gives an overall 33% fluorescence decrease and an apparent K_D' of 2.6 ± 0.3 mM phosphate. [In contrast, the fluorescence of NATA under the same conditions shows only ~5% quench by 50 mM sodium phosphate.] Following the addition of 28 mM sodium phosphate to HD(wt) at which concentration no further quench in fluorescence occurs, the addition of an equal molar quantity of "recognition-site, sequence-specific" 28 bp DNA to HD(wt) produces a fluorescence increase of 19% (after correcting for inner filter effects caused by light absorption by DNA). Thus, the quenching of the intrinsic Trp48 fluorescence by phosphate is partially reversed by DNA binding (data not shown). The quench of Trp48 fluorescence by phosphate may be a local effect since the addition of NaCl, which also stabilizes vnd/NK-2 homeodomains, has no effect on Trp48 fluorescence.

Representative second derivative UV absorption spectra at 25 and 65 °C reveal changes in the environment of Tyr and Trp residues during thermal unfolding of HD(wt) in either 50 mM sodium phosphate or 50 mM Hepes/500 mM NaCl, pH 7.4, buffer (Figure 5). Changes in the peak-trough at ~287−283 nm (a) represent mainly Tyr exposure with some contributions from Trp whereas those at ~293−290 nm (b) represent mainly Trp environmental changes (*23*, *24*). The ratio of $a/b = R_N$ for the native, folded protein and $a/b = R_U$ for the unfolded protein, and these parameters have been used by Ragone et al. (*23*) to estimate the degree of exposure of Tyr in proteins: $\alpha = (R_N - R_0)/(R_U - R_0)$, where R_0 is a reference state for the protein in ethylene glycol ($R_0 \cong -0.10$). Using this relationship for the HD(wt) protein (with a Tyr/Trp ratio of 4/1), values of α for the degree of exposure of Tyr at 25 °C are ~0.78 (3.2 Tyr) and 0.87 (3.5 Tyr) in Hepes/NaCl and sodium phosphate buffer, respectively. This means that >75% of the Tyr residues in the vnd/NK-2 homeodomain are solvent accessible in the native, folded form, although phosphate produces subtle differences in the second derivative spectrum (Figure 5). Comparison

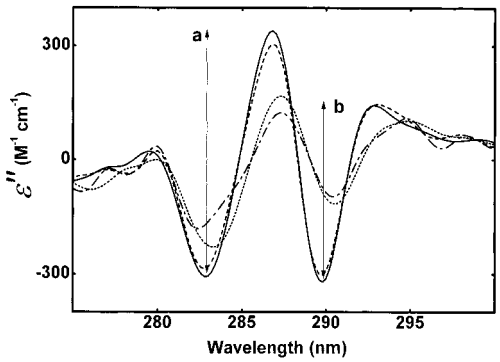

FIGURE 5: Second derivative UV spectra for folded and unfolded forms of HD(wt). Spectra (ϵ'') are given in the units M^{-1} cm^{-1} and were obtained with 24 μM HD(wt) in 50 mM Hepes/500 mM NaCl, pH 7.4 (solid line at 25 °C and dotted line at 65 °C), and with 15 μM HD(wt) in 50 mM sodium phosphate, pH 7.4 (dashed line at 25 °C and dot-dashed line at 65 °C). Peak-through amplitudes *a* and *b* are indicated by vertical lines at 283 and 290 nm, and the ratios ($R_{a/b}$) are 1.4 (25 °C) and 1.8 (65 °C) in Hepes and 1.3 (25 °C) and 1.5 (65 °C) in sodium phosphate.

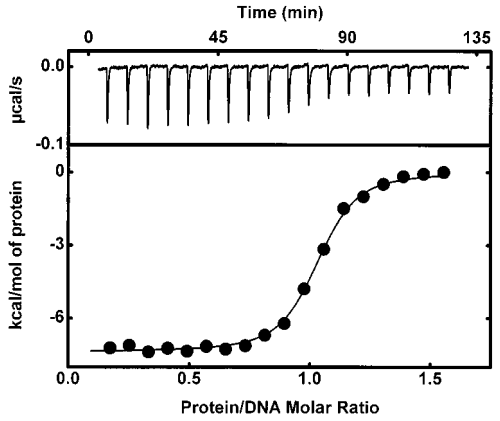

FIGURE 6: Representative titration of sequence-specific 18 bp duplex DNA with wild-type vnd/NK-2 homeodomain in 50 mM sodium phosphate, pH 7.4, buffer at 25 °C. The DNA concentration in the ITC sample cell is 1.63 μM, and 35.3 μM HD(wt) is in the syringe. Upper panel: Observed heats (after instrument equilibration) for 2−18 injections of 5 μL protein additions at 7 min intervals after baseline correction. Heats of dilution for protein are obtained from injections 17−18 and subtracted from the data. Lower panel: Corrected, normalized binding enthalpies vs protein/DNA molar ratios are shown. Injections 2−9 give the binding enthalpy at saturating DNA. The data (●) are fitted to a one-site binding model (—) which give $K_A' = 1.2 \pm 0.1 \times 10^8$ M^{-1}, $\Delta H = -7.2 \pm 0.1$ kcal mol^{-1}, and $n = 0.998$ for the stoichiometry of HD(wt) binding to specific duplex DNA.

of the magnitudes of the *b* peak-trough at 25 and 65 °C in Figure 5 indicates that $\Delta\epsilon_{max}'' \cong 240$ M^{-1} cm^{-1} for Trp48 exposure during thermal unfolding in either Hepes or phosphate buffer. This is the same value within the error of this method as that previously found for the maximum change in Trp exposure during thermally induced exposure of a single Trp in an unrelated protein (*31*).

Thermodynamics of Binding Sequence-Specific Double-Stranded DNA. A representative ITC experiment in which injections of 0.177 μmol of HD(wt) per 5 μL addition into 1.63 μM sequence-specific 18 bp duplex DNA at 25 °C in 50 mM sodium phosphate, pH 7.4, is shown in Figure 6. Under these conditions, the enthalpy of binding DNA is obtained from the second through ninth additions of protein to DNA, and the signal decreases after the ninth addition of

Table 2: Enthalpies for vnd/NK-2 Homeodomains Binding Sequence-Specific Duplex DNA at pH 7.4 under Different Conditions[a]

protein	buffer	temp (°C)	ΔH (kcal mol^{-1})	*N*
HD(wt)	A	10	−10.8 ± 0.2	3
		15	−8.1 ± 0.2	5
		20	−7.9 ± 0.1	13
		20	−7.7 ± 0.2	7[b]
		25	−7.2 ± 0.1	8
		30	−5.1 ± 0.1	5
	B	10	−10.6 ± 0.4	14
	C	10	−10.1 ± 0.1	10[b]
		20	−7.6 ± 0.1	8[b]
HD(H52R)	A	10	−8.1 ± 0.1	10
		15	−9.3 ± 0.2	19
		20	−10.3 ± 0.2	13
		25	−10.9 ± 0.2	10
HD(H52R/T56W)	A	10	−7.5 ± 0.2	7
		25	−9.0 ± 0.6	12

[a] From initial injections of protein into saturating concentrations of 18 bp duplex DNA (unless otherwise indicated) in the VP-ITC at the indicated temperatures. Concentrations of stock protein were 35−65 μM, and DNA was 0.9−1.6 μM in the ITC cell. Stoichiometry of protein-DNA interaction was 1.0 ± 0.1. Values of ΔH at saturating DNA, the standard deviation from the mean, and the total number of injections from one to three titrations (*N*) are given for each condition. Buffers at pH 7.4 were as follows: A, 50 mM sodium phosphate; B, 50 mM Hepes; C, 50 mM Hepes/100 mM NaCl. [b] Sequence-specific 28 bp duplex DNA was used.

HD(wt) since all of the DNA has been complexed by the homeodomain. The areas for the heat of dilution of protein, which are the same as obtained by adding HD(wt) to buffer, are obtained from the 17−18th additions in Figure 6, and this value is subtracted from the areas for injections 2−16 of protein. A fit of corrected enthalpy values (Figure 6, lower panel) gives a stoichiometry $n = 0.998$, $K_A' = 1.2 \pm 0.1 \times 10^8$ M^{-1}, and $\Delta H = -7.2 \pm 0.1$ kcal/mol for HD(wt) binding DNA under the conditions used. The availability of the more sensitive VP-ITC than that of the prior model [MC2 Omega ITC from MicroCal, Inc.] used by Carra and Privalov (*32*) allows measurements of association constants of 10^4-10^9 M^{-1}.

Titrations of either 18 or 28 bp specific DNA by HD(wt) at different temperatures [at which HD(wt) is folded] and in different buffers also have been performed. Average values of ΔH obtained at saturating DNA together with standard errors of the mean and the total number of injections are summarized in Table 2. Within experimental error, binding enthalpies for HD(wt) interacting with DNA are the same in either sodium phosphate or 50 mM Hepes ± 100 mM NaCl at the same temperature. This indicates an absence of a net proton uptake or release in the binding of DNA by HD(wt), since the heat of protonation of Hepes is ~9-fold that of phosphate. Moreover, approximately the same binding enthalpies are obtained with either the 18 bp or 28 bp duplex DNA containing the specific 5′-CAAGTG-3′ binding sequence in the core.

Comparable data for titrations of 18 bp specific duplex DNA with HD(H52R) and HD(H52R/T56W) in 50 mM sodium phosphate, pH 7.4, are given also in Table 2. In all cases, the stoichiometry of homeodomain binding DNA is 1.0 ± 0.1. Association constants of $1.20 \pm 0.15 \times 10^8$ M^{-1} and $1.95 \pm 0.75 \times 10^8$ M^{-1} have been obtained for HD(H52R) and HD(H52R/T56W), respectively, binding DNA at 25 °C in 50 mM sodium phosphate (pH 7.4).

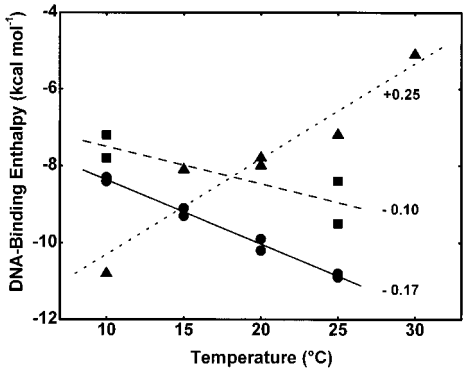

FIGURE 7: Enthalpy changes for vnd/NK-2 homeodomains binding sequence-specific 18 bp duplex DNA in 50 mM sodium phosphate, pH 7.4, as a function of the temperature of the ITC measurements. Shown are average ΔH values at saturating DNA from separate titrations of DNA: ▲, HD(wt); ●, HD(H52R); ■, HD(H52R/T56W). Under these conditions, T_m values for protein unfolding are ≥48 °C (Table 1). Each data set has been fit by linear least squares, and the slope (ΔC_p) values are shown.

Figure 7 shows ΔC_p plots of ΔH values from *different* titration experiments with 18 bp duplex DNA and HD(wt), HD(H52R), and HD(H52R/T56W) in 50 mM sodium phosphate, pH 7.4, buffer at different temperatures. Values of ΔC_p have been obtained by linear least-squares fitting of the ΔH values at the different temperatures for each homeodomain binding DNA. The slopes of the plots in Figure 7 give the ΔC_p values and SD errors shown in Table 3. These heat capacity changes are much smaller than usually observed for protein interactions with specific DNA (*33, 34;* see below).

Dissociation constants for the same proteins [HD(wt), HD(H52R), and HD(H52R/T56W)] binding to sequence-specific 18 bp DNA have been determined by Weiler et al. (*8*) from gel mobility shift assays at 4 °C to be $1.0 \pm 0.5 \times 10^{-9}$ M^{-1}. This value and the values of ΔH and ΔC_p determined here for the these homeodomains binding specific DNA at 25 °C give calculated $\Delta G'$ values at 298 K of -11.6 ± 0.3, -11.6 ± 0.3, and -11.7 ± 0.3 kcal mol^{-1} for HD(wt), HD(H52R), and HD(H52R/T56W) binding DNA, respectively. These calculated values of $\Delta G'$ are somewhat more negative than measured here (Table 3), but electrophoresis buffers and other conditions differ from what has been used in the present studies. Moreover, both free and DNA-bound protein are in equilibrium in ITC measurements.

Table 3 summarizes thermodynamic parameters for HD(wt), HD(H52R), and HD(H52R/T56W) binding sequence-specific 18 bp duplex DNA at 298 K in 50 mM sodium phosphate at pH 7.4. In all cases, DNA binding reactions are enthalpically controlled at 298 K with smaller, positive values of $T\Delta S$ than negative binding enthalpies, where $\Delta G' = \Delta H - T\Delta S$. For completeness, ΔC_p values (see above) are given also in Table 3. The sign and magnitude of $T\Delta S$ values are unexpected in view of the ordering of the vnd/NK-2 homeodomains HD(wt) and HD(H52R) that occurs upon DNA binding (*14*). HD(H52R/T56W) has a longer helix III in the free state than does HD(wt) or HD(H52R) (*8*), and yet the $T\Delta S$ value is only ∼one-half that of the wild-type homeodomain. Thus, the solvent contribution to the DNA−homeodomain interactions must have an important role.

DISCUSSION

For thermal unfolding of vnd/NK-2 homeodomains, T_m values from DSC and far-UV−CD measurements agree (Table 1). Changes in secondary structure during thermally induced unfolding of HD(wt) (Figure 2), HD(H52R), and HD(H52R/T56W) show ideal two-state behavior although differences in the cooperativity of unfolding are evident, as has been observed by Weiler et al. (*8*). Equilibrium CD measurements give the same results. In contrast, DSC data require a non-two-state model for fitting endotherms (Figure 3). The presence of phosphate or NaCl increases the cooperativity of CD transitions, and for HD(H52R) and HD(H52R/T56W) in 100 mM NaCl, enthalpic values for CD transitions approximate ΔH_{vH} values calculated form DSC data. Usually there is agreement between ΔH_{cal} from DSC and far-UV ellipticity changes for thermal unfolding of small globular proteins, but this is not the case for vnd/NK-2 homeodomains. Although both methods monitor unfolding transitions in proteins, DSC measurements reflect predominantly changes in the hydration of hydrophobic residues whereas far-UV CD is most sensitive to changes in helix content.

DSC results for the thermal unfolding of the wild-type vnd/NK-2 homeodomain at pH 7.4 give a cooperative ratio ($\Delta H_{cal}/\Delta H_{vH}$) less than unity under all conditions (Table 1). For thermal unfolding of HD(H52R) and HD(H52R/T56W) in the presence of 100 mM NaCl, cooperative ratios of ∼0.8 are observed. That is, endotherms have narrower temperature ranges than expected for ideal two-state unfolding (Figure 3). The usual explanation for a cooperativity ratio less than unity is that intermolecular interactions occur during unfolding. However, the absence of posttransitional baseline shifts, the reliability of baselines, and the repeatability of DSC scans suggest that any intermolecular interactions at high temperatures are not irreversible such as those leading to aggregation. Moreover, NMR studies have not detected any dimerization or higher aggregates of vnd/NK-2 homeodomains even though >10-fold higher concentrations of protein are present in NMR than in DSC measurements. The reversibility of transitions (Figure 3), the similarity in calculated ΔH_{vH} values from DSC data (47 ± 5 kcal mol^{-1}) for all proteins under different conditions, the variation in ΔH_{cal} values, and the noncorrelation between DSC and CD data suggest that we seek an alternative explanation for ratios of $\Delta H_{cal}/\Delta H_{vH}$ being less than unity for vnd/NK-2 homeodomains. One possibility might involve unusual intramolecular tertiary structure interactions that influence DSC endotherm shapes below and above transition temperatures. The substitution of His52 by Arg, which markedly stabilizes the vnd/NK-2 homeodomain [presumably by bridging helices I and III (*8*)], increases the cooperative ratio (Table 1). Thus, the length and flexibility of helix III of the vnd/NK-2 homeodomain (*8*) appear to affect the unfolding and refolding of tertiary structure. Studies of scan rate dependence, which might detect such behavior, are necessarily limited by the small signal [1.1−3.4 cal/g for HD(wt); Table 1] and the instability of proteins during prolonged exposure to high temperatures, for which reasons only 30 and 60 °C/h scan rates have been examined.

The NMR solution structure of the wild-type vnd/NK-2 homeodomain determined by Tsao et al. (*15*) indicates that

Table 3: Thermodynamic Parameters for vnd/NK-2 Homeodomains Binding Sequence-Specific 18 bp Duplex DNA in 50 mM Sodium Phosphate, pH 7.4 at 298 K[a]

	$\Delta G'$ (kcal mol^{-1})	ΔH^b (kcal mol^{-1})	$T\Delta S$ (kcal mol^{-1})	$\Delta C_p{}^c$ (kcal K^{-1} mol^{-1})
HD(wt)	-11.0 ± 0.1	-6.6 ± 0.5	$+4.4 \pm 0.5$	$+0.25 \pm 0.04$
HD(H52R)	-11.0 ± 0.1	-10.8 ± 0.1	$+0.2 \pm 0.1$	-0.17 ± 0.01
HD(H52R/T56W)	-11.3 ± 0.3	-9.0 ± 0.6	$+2.3 \pm 0.6$	-0.10 ± 0.04

[a] From ITC titrations in which the stoichiometry of homeodomains binding DNA is 1.0 ± 0.1 (see text). [b] Values of ΔH at 298 K are from linear least-squares fitting of ΔH values vs temperature (Figure 7). [c] From the slopes of the plots in Figure 7 with linear least-squares errors in the fits of the data.

a salt bridge between Arg19 (helix I) and Glu30 (helix II) is present together with hydrogen bonds between the backbone of Arg24 (first loop) and the Arg53 side chain (helix III). An unusual His in position 52 of the vnd/NK-2 homeodomain [usually occupied by Arg in most homeodomain proteins; see Gehring et al. (*1*)] precludes the formation of a salt bridge between Glu17 and residue 52. In fact, the HD(H52R) protein has an ion pair interaction that bridges Glu17 (helix I) and Arg52 (helix III) (*8*), and yet the cooperative ratio for unfolding is less than unity as it is for the wild-type homeodomain. In contrast, DSC studies of Carra and Privalov (*32*) on the thermal unfolding of the yeast MATα2 homeodomain (which has an Arg residue at the fourth position downstream from the conserved Trp in the DNA binding region) show that this protein has a cooperative ratio equal to unity under a variety of conditions. Nevertheless, CD measurements at 222 nm for the unfolding of MATα2 do not agree with ΔH_{cal} values. In this case, the authors estimate that residues 50−58 of the MATα2 helix III in the DNA recognition site are unfolded in the free state and measure $\Delta H_{cal} = 33$ kcal mol^{-1} (3.3 cal/g) for thermal unfolding of this homeodomain in 20 mM sodium phosphate (pH 7.0) in the absence of NaCl, which is ~1.6-fold greater than that measured by DSC here for the thermal unfolding of HD(H52R). Clearly, the behavior of the vnd/NK-2 homeodomain in DSC studies of thermal unfolding differs from that of MATα2 due possibly to differences in tertiary structure.

The presence of 50 mM sodium phosphate at pH 7.4 significantly stabilizes the vnd/NK-2 homeodomain [HD(wt), HD(H52R), and HD(H52R/T56W)] with T_m increases of ~13 °C in reference to T_m values observed for the same proteins in 50 mM Hepes, pH 7.4 (Table 1). The stabilization by phosphate appears to be due to specific binding, and the quench of Trp48 produced by phosphate binding is partially reversed by adding a stoichiometric amount of sequence-specific DNA. This observation supports the idea that phosphate binds to some homeodomain sites that interact with the phosphates of DNA, and one likely site is Arg53 with an involvement of Tyr54 in both the quench of Trp48 fluorescence and interactions with duplex DNA. The presence of NaCl also increases the stability and reversibility of unfolding transitions of vnd/NK-2 homeodomains (Table 1; Figure 2). Since vnd/NK-2 homeodomains have a net positive charge, the effects of NaCl relate to electrostatic factors during unfolding/refolding. However, comparing the conformational stabilities of HD(H52R) and HD(H52R/T56W) to that of HD(wt), T_m values of the former are higher than that of HD(wt) irrespective of the presence of phosphate or NaCl.

Upon binding to duplex 18 bp DNA (B-form) containing the specific 5′-CAAGTG-3′ binding sequence in its central region, the wild-type vnd/NK-2 homeodomain protein (helix−turn−helix structural motif) undergoes several changes in both side chain and secondary structural organization [Gruschus et al. (*16*); Figure 8]. Both N- and C-terminal regions become more ordered upon DNA binding; several interactions between amino acid residues and DNA bases are formed, and various contacts are made between Arg5 and Leu7 in the N-terminal segment with the minor groove of DNA. Also, interactions between Arg53 and Asn51 (both in helix III) with the DNA backbone and significant hydrophobic contacts between Ile47 and Tyr54 with deoxyribose rings in the major groove have been identified by NMR spectroscopy. Moreover, a remarkable increase in the length of helix III (from 11 to 19 amino acid residues) upon binding to specific duplex DNA has been reported by Tsao et al. (*14*).

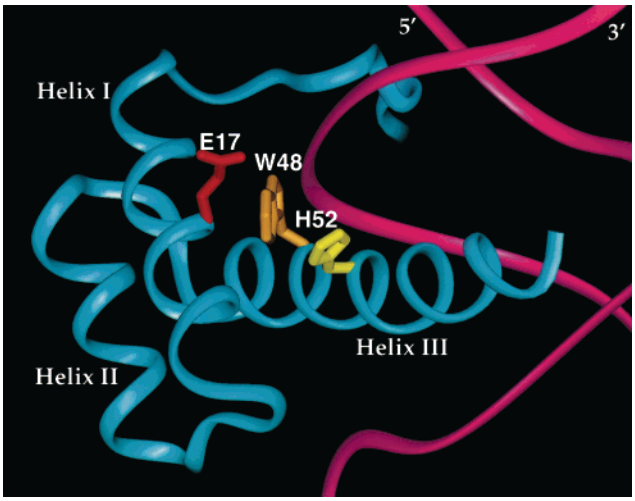

FIGURE 8: Close-up view of the HD(wt)/$^{d/s}$DNA complex from the NMR solution structure of Gruschus et al. (*16*). The helix−turn−helix motif of the vnd/NK-2 homeodomain is shown in blue, and the DNA strands are in pink with the 3′ and 5′ ends labeled. The "recognition-site" helix (III) is inserted into the center of the major groove of the DNA structure. Backbone structures of Glu17, Trp48, and His52 are shown to display relative positions.

A large negative heat capacity change is usually associated with site-specific binding of proteins to DNA, as summarized by Spolar and Record (*33*) and Privalov et al. (*34*). A coupling of local protein folding, in which the burial of apolar surfaces has a dominant role, can account for observed negative ΔC_p values (*33*). Despite the fact that helix III of the wild-type vnd/NK-2 is elongated upon binding to DNA (*14*), the observed value of ΔC_p is small and positive (+0.25 kcal K^{-1} mol^{-1}), as determined here by isothermal titration calorimetry from 10 to 30 °C under which conditions HD(wt) is folded. Thus, this appears to be an exceptional case in which a decrease in the solvent-accessible, hydrophobic surfaces produced by DNA binding is offset by solvent

rearrangement, burial of polar surfaces, and possibly a strain in the duplex DNA conformation. Although ΔC_p values for HD(H52R) and HD(H52R/T56W) binding specific duplex DNA are negative (−0.17 and −0.10, respectively), their magnitude is considerably less than predicted from changes in surface-exposed areas that occur upon binding.

From the values of ΔH determined by ITC at 10−30 °C for HD(wt) binding 18 bp duplex DNA in 50 mM sodium phosphate at pH 7.4, $\Delta H = -6.6$ kcal mol^{-1} for this binding reaction at 298 K. Under the same conditions, $\Delta H \cong -10.8$ and −9.0 kcal mol^{-1} at 298 K for HD(H52R) and HD(H52R/T56W), respectively, binding 18 bp duplex DNA (Table 3). Enthalpic changes and $\Delta G'$ values obtained from ITC titrations under the same conditions indicate that for vnd/NK-2 homeodomain proteins binding sequence-specific duplex DNA, reactions are enthalpically controlled. Corresponding ΔS values are approximately +15, +1, and +8 cal K^{-1} mol^{-1} for HD(wt), HD(H52R), and HD(H52R/T56W) proteins binding sequence-specific 18 bp duplex DNA at pH 7.4 and 298 K.

Enthalpic changes for the interaction of HD(wt) with specific, double-stranded DNA are the same in 50 mM Hepes ± 100 mM NaCl as in 50 mM sodium phosphate at pH 7.4, suggesting that a net proton uptake or release is not involved upon complex formation.

On the basis of the behavior of just the homeodomains upon binding DNA, the entropy changes are somewhat surprising. One might have expected a large negative entropy for the binding of HD(wt) and HD(H52R) to DNA as a penalty to be paid for elongation of helix III upon binding and a much smaller entropy change for HD(H52R/T56W) binding to DNA since, in this case, helix III is elongated in the free state before binding to DNA (*8*, *14*). The observed behavior does not follow this order, presumably due to large contributions from solvent rearrangements and other factors. Nevertheless, it is remarkable that the overall entropy changes for these binding reactions are small considering the large entropy factors that are involved (*33*, *34*). The origin of entropy changes associated with vnd/NK-2 homeodomain binding DNA deserves considerable attention in future studies. If, for example, the vnd/NK-2 homeodomain exists as a heterodimer with an as yet unidentified protein, thermodynamic parameters for binding sequence-specific duplex DNA possibly will be altered.

ACKNOWLEDGMENT

The authors appreciate the assistance of Kimberley Marshall-Batty in the laboratory of Dr. Henry M. Fales (LBC, NHLBI) in performing mass spectral analysis on vnd/NK-2 homeodomain recombinant proteins. Also, we thank James M. Gruschus (LBC, NHLBI) for help in depicting the main structural features of the vnd/NK-2 homeodomain−DNA complex in Figure 8 and for proton NMR measurements of 18 bp duplex DNA.

REFERENCES

1. Gehring, W. J., Affolter, M., and Bürglin, T. (1994) *Annu. Rev. Biochem. 63*, 487−526.
2. McGinnis, W., and Krumlauf, R. (1992) *Cell 68*, 283−302.
3. Scott, M. P., Tamkun, J. W., and Hartzell, G. W. (1989) *Biochim. Biophys. Acta 989*, 25−48.
4. Boncinelli, E. (1997) *Curr. Opin. Genet. Dev. 7*, 331−337.
5. de Kok, Y. J., Cremers, C. W., Ropers, H. H., and Cremers, F. P. (1997) *Hum. Mutat. 10*, 207−211.
6. Morell, R., Carey, M. L., Lalwani, A. K., Friedman, T. B., and Asher, J. H. (1997) *Hum. Hered. 47*, 38−41.
7. Schott, J. J., Benson, D. W., Basson, C. T., Pease, W., Silberbach, G. M., Moak, J. P., Maron, B. J., Seidman, C. E., and Seidman, J. G. (1998) *Science 281*, 108−111.
8. Weiler, S., Gruschus, J. M., Tsao, D. H. H., Yu, L., Wang, L. H., Nirenberg, M., and Ferretti, J. A. (1998) *J. Biol. Chem. 273*, 10994−11000.
9. Xiang, B., Weiler, S., Nirenberg, M., and Ferretti, J. A. (1998) *Proc. Natl. Acad. Sci. U.S.A. 95*, 7412−7416.
10. Tucker-Kellogg, L., Rould, M. A., Chambers, K. A., Ades, S. E., Sauer, R. T., and Pabo, C. O. (1997) *Structure 5*, 1047−1057.
11. Kim, Y., and Nirenberg, M. (1989) *Proc. Natl. Acad. Sci. U.S.A. 86*, 7716−7720.
12. Jimenez, F., Martin-Morris, L. E., Valasco, L., Chu, H., Sierra, J., Rosen, D. R., and White, K. (1995) *EMBO J. 14*, 3487−3495.
13. Nirenberg, M., Nakayama, K., Nakayama, N., Kim, Y., Mellerick, D., Wang, L. H., Webber, K., and Lad, R. (1995) *Ann. N.Y. Acad. Sci. 758*, 224−242.
14. Tsao, D. H. H., Gruschus, J. M., Wang, L. H., Nirenberg, M., and Ferretti, J. A. (1994) *Biochemistry 33*, 15053−15060.
15. Tsao, D. H. H., Gruschus, J. M., Wang, L. H., Nirenberg, M., and Ferretti, J. A. (1995) *J. Mol. Biol. 251*, 297−307.
16. Gruschus, J. M., Tsao, D. H. H., Wang, L. H., Nirenberg, M., and Ferretti, J. A. (1999) *J. Mol. Biol. 289*, 529−545.
17. Novagen (1995) *pET System Manual*, 6th ed., Novagen, Madison, WI.
18. Perkins, S. J. (1986) *Eur. J. Biochem. 157*, 169−180.
19. Plotnikov, V. V., Brandts, J. M., Lin, L. N., and Brandts, J. F. (1997) *Anal. Biochem. 250*, 237−244.
20. Ginsburg, A., and Zolkiewski, M. (1991) *Biochemistry 30*, 9421−9429.
21. Kirchhoff, W. H. (1993) *NIST Technical Note 1401*: *EXAM* (CODEN: NTNOEF) U.S. Government Printing Office, Washington, DC.
22. MicroCal, Inc. (1998) *VP-ITC Microcalorimeter User's Manual*, MicroCal, Inc., Northampton, MA.
23. Ragone, R., Colonna, G., Balestrieri, C., Servillo, L., and Irace, G. (1984) *Biochemistry 23*, 1871−1875.
24. Shrake, A., Fisher, M. T., McFarland, P. J., and Ginsburg, A. (1989) *Biochemistry 28*, 6281−6294.
25. Lakowicz, J. R. (1999) in *Principles of fluorescence spectroscopy* (Kluwer, Ed.) 2nd ed., Academic/Plenum Publishers, New York.
26. Ginsburg, A., Gorman, E. G., Neece, S. H., and Blackburn, M. B. (1987) *Biochemistry 26*, 5989−5996.
27. Damante, G., Tell, G., Leonardi, A., Fogolari, F., Bortolotti, N., Di Lauro, R., and Formisano, S. (1994) *FEBS Lett. 354*, 293−296.
28. Sanchez-Ruiz, J. M., Lopez-Lacomba, J. L., Cortijo, M., and Mateo, P. L. (1988) *Biochemistry 27*, 1648−1652.
29. Freire, E., van Osdol, W. W., Mayorga, O. L., and Sanchez-Ruiz, J. M. (1990) *Annu. Rev. Biophys. Biophys. Chem. 19*, 159−188.
30. Privalov, P. L., and Khechinashvili, N. N. (1974) *J. Mol. Biol. 86*, 665−684.
31. Zolkiewski, M., and Ginsburg, A. (1992) *Biochemistry 31*, 11991−12000.
32. Carra, J. H., and Privalov, P. L. (1997) *Biochemistry 36*, 526−535.
33. Spolar, R. S., and Record, M. T., Jr. (1994) *Science 263*, 777−784.
34. Privalov, P. L., Jelesarov, I., Read, C. M., Dragan, A. I., and Crane-Robinson, C. (1999) *J. Mol. Biol. 294*, 997−1013.

BI0022341